NIH Public Access
Author Manuscript
J Immunol. Author manuscript; available in PMC 2013 January 15.

Published in final edited form as:
J Immunol. 2012 January 15; 188(2): 649–660. doi:10.4049/jimmunol.1003845.

IL-10 Limits Parasite Burden and Protects against Fatal Myocarditis in a Mouse Model of *Trypanosoma cruzi* Infection

Ester Roffê[*], **Antonio Gigliotti Rothfuchs**[†,‡], **Helton C. Santiago**[§], **Ana Paula M. P. Marino**[*], **Flavia L. Ribeiro-Gomes**[¶], **Michael Eckhaus**[‖], **Lis R. V. Antonelli**[†,#], and **Philip M. Murphy**[*]

[*]Molecular Signaling Section, Laboratory of Molecular Immunology, National Institute of Allergy and Infectious Diseases (NIAID), National Institutes of Health (NIH), Bethesda, MD, USA

[†]Immunobiology Section, Laboratory of Parasitic Diseases, NIAID/NIH, Bethesda, MD, USA

[‡]Department of Microbiology, Tumor and Cell Biology, Karolinska Institutet, Stockholm, Sweden

[§]Helminth Immunology Section, Laboratory of Parasitic Diseases, NIAID/NIH, Bethesda, MD, USA

[¶]Intracellular Parasite Biology Section, Laboratory of Parasitic Diseases, NIAID/NIH, Bethesda, MD, USA

[‖]Division of Veterinary Resources, Office of Research Services, Office of the Director, NIH, Bethesda, MD, USA

[#]Laboratory of Immunopathology, René Rachou Research Center, FIOCRUZ, Belo Horizonte 30190-002, MG, Brazil

Abstract

Chagas' Disease is a zoonosis prevalent in Latin America caused by the protozoan *Trypanosoma cruzi*. The immunopathogenesis of cardiomyopathy, the main clinical problem in Chagas' Disease, has been extensively studied but is still poorly understood. Here we systematically compared clinical, microbiologic, pathologic, immunologic and molecular parameters in two mouse models with opposite susceptibility to acute myocarditis caused by the myotropic Colombiana strain of *T. cruzi*: C3H/HeSnJ (100% mortality, uncontrolled parasitism) and C57BL/6J (<10% mortality, controlled parasitism). *T. cruzi* induced differential polarization of immunoregulatory cytokine mRNA expression in the hearts of C57BL/6J versus C3H/HeSnJ mice, however most differences were small. The difference in IL-10 expression was exceptional (C57BL/6J 8.7-fold > C3H/HeSnJ). Consistent with this, hearts from infected C57BL/6J mice, but not C3H/HeSnJ mice, had a high frequency of total IL-10-producing $CD8^+$ T cells and both $CD4^+$ and $CD8^+$ subsets of $IFN\gamma^+IL\text{-}10^+$ double-producing T cells. Furthermore, *T. cruzi* infection of $IL\text{-}10^{-/-}$ C57BL/6J mice phenocopied fatal infection in wild type C3H/HeSnJ mice with complete loss of parasite control. Adoptive transfer experiments indicated that T cells were a source of protective IL-10. Thus, in this system IL-10 production by T cells promotes *T. cruzi* control and protection from fatal acute myocarditis.

Keywords

Parasitic-protozoan; cytokines; T cells; inflammation

Corresponding Author: Philip M. Murphy, M. D., 9000 Rockville Pike, MSC-1888, Bldg. 10, Room 11N113, NIH, Bethesda, MD 20892; Tel: 301-496-8616; Fax: 301-402-4369; pmm@nih.gov.

NIH-PA Author Manuscript
NIH-PA Author Manuscript
NIH-PA Author Manuscript

NIH-PA Author Manuscript
NIH-PA Author Manuscript
NIH-PA Author Manuscript

Introduction

Chagas' Disease is a vector-borne zoonosis restricted to Latin America caused by infection with the protozoan *Trypanosoma cruzi*. The prevalence of Chagas' Disease remains high, approximately 10 million in the year 2006 according to estimates by the World Health Organization [1], in part due to inadequate implementation of vector and blood supply control programs. Currently, there is no vaccine available and the few approved drugs are of limited use due to serious side-effects and limited efficacy [2]. Risk factors and immunopathogenic mechanisms in *T. cruzi* infection are poorly understood. The acute phase is usually short and subclinical, but over time ~20-30% of patients progress to clinically evident Chagas' Disease, mainly manifest as dilated cardiomyopathy [3].

Consistent with the intracellular lifestyle of *T. cruzi*, studies in animal models and with human subjects strongly suggest that it induces a Th1-polarized immune-mediated process in affected organs [4]. Mice genetically deficient in the signature Th1 cytokines IL-12 or IFNγ, the IFNγ–induced effector enzyme iNOS [5], the Th1-associated chemokine receptors CCR2 [6] or CCR5 [7], and the Th1-associated ligands for chemokine receptor CXCR3 [8] all develop increased parasitism after infection, and some have high acute mortality. Persistent parasitism and type 1 responses may promote progression to the chronic phase. In animal models of chronic infection, parasite DNA and antigens are still found in infected tissues in the presence of cell infiltration and fibrosis, indicating an inappropriate or ineffective immune response. In chronic human *T. cruzi* infection, the cytokine profile in the heart is also Th1-polarized [9], and PBMCs produce high levels of IFNγ and low levels of IL-10 [10].

A problem in interpreting results from mouse models of *T. cruzi* infection is that many different models have been used with many different parasite strains and inocula and diverse mouse strains, with variable outcomes from the many labs working in the field. In the present study, we have systematically and directly compared the clinical, parasitologic, pathologic, immunologic and molecular correlates of infection using the myotropic Colombiana strain of *T. cruzi* [11] in two experimental mouse models with opposite outcomes: C57BL/6J, which control parasitism and survive infection, and C3H/HeSnJ, which fail to control parasitism and die. This approach allowed us to identify a strong association of IL-10 and IL-10-producing cells with resistance and to test the functional importance of IL-10 directly using gene knockout mice and adoptive transfer experiments. This confirms previous reports of IL-10 as a protective factor in *T. cruzi* infection [12-15] and provides new insights with regard to the source of IL-10 and its effects on parasitism.

Materials and Methods

Animals and Parasite

The following mice were obtained from Jackson Laboratory (Bar Harbor, ME): Wild type male C57BL/6J mice (stock number 664); wild type male C3H/HeSnJ mice (stock number 661); IL-10 deficient male mice (stock number 2251, backcrossed for 10 generations onto the C57BL/6J background); RAG-1 deficient male mice (stock number 2216, backcrossed for 10 generations onto the C57BL/6J background); C3.SW-H2b/SnJ male mice (stock number 0438); and C3H/HeJ male mice (stock number 659). Inbred wild type male C3H/HeN mice and wild type male C57BL/6N mice were obtained from Taconic Farms (Hudson, NY). Parasitemia and mortality were similar after *T. cruzi* infection of the C57BL/6 and C3H/He lines obtained from Jackson and from Taconic Farms (not shown). Mice were infected at 8-10 wks of age and housed in cages under specific pathogen-free conditions. All animals were used under the auspices of a protocol approved by the National Institute of Allergy and Infectious Diseases Animal Care and Use Committee. The myotropic

NIH-PA Author Manuscript

NIH-PA Author Manuscript

NIH-PA Author Manuscript

Colombiana strain of *Trypanosoma cruzi*, obtained from Dr. Fuyuki Tokumasu and Dr. James Dvorak (Laboratory of Malaria and Vector Research, NIAID/NIH) was maintained by serial passage in Swiss Webster mice (Taconic Farms) every 21 days. Animals were infected intraperitoneally with 1,000 blood-stage trypomastigote forms of *T. cruzi*. Parasitemia levels were determined by light microscopy by counting the number of parasites in an unstained 5 μl drop of whole blood drawn from the tail vein and mounted between a microscope slide and cover slip at 400X magnification, as described [16].

mRNA Analysis

Real-time RT-PCR was performed as previously described [17], with minor modifications, using tissues from infected and control mice. Total RNA was isolated from hearts using an RNeasy kit (Qiagen, Valencia, CA) and real-time RT-PCR was performed on an ABI PRISM 7900 sequence detection system (Applied Biosystems, Foster City, CA) using SYBR Green PCR Master Mix (Applied Biosystems) after reverse transcription of 1 μg RNA using M-MLV reverse transcriptase (Promega, Madison, WI). The relative level of gene expression was determined by the comparative threshold cycle method as described by the manufacturer, in which data for each sample were normalized to hypoxanthine phosphoribosyltransferase (HPRT), and expressed as fold-change compared with uninfected controls. The primer sequences are available upon request.

Quantification of Parasite Tissue Loads by Real-Time PCR

Real-time PCR was performed as described previously [18], with minor modifications. Briefly, on different days after infection, DNA was extracted from heart, spleen and liver using a DNeasy kit (Qiagen). Real-time PCR using 50 ng of total DNA was performed on an ABI PRISM 7900 sequence detection system using SYBR Green PCR Master Mix according to the manufacturer's recommendations. The level of host DNA was determined by measurement of genomic IL-12 p40 PCR product levels in the same samples. Purified *T. cruzi* DNA, obtained from trypomastigote cultures maintained *in vitro*, was sequentially diluted for standard curve generation in aqueous solution containing equivalent amounts of DNA from uninfected mouse tissues. The following *T. cruzi* specific-primers were used, targeting a 195-bp repeat in the TCZ region: 5′-GCTCTTGCCCACAMGGGTGC-3′ (forward), where M = A or C, and 5′-CCAAGCAGCGGATAGTTCAGG-3′ (reverse). The genomic IL-12 p40-specific primers were: 5′-GTAGAGGTGGACTGGACTCC-3′ (forward) and 5′-CAGATGTGAGTGGCTCAGAG-3′ (reverse).

Histopathological Analysis

Mouse organs were removed and washed in sterile PBS. Immediately after drying the surfaces by tamping with absorbent paper, organs were fixed in 4% buffered paraformaldehyde and processed for paraffin embedding. Six μm thick sections were cut with a microtome, then stained with hematoxylin and eosin to investigate inflammation and parasitism, or with Gomori's Trichrome to assess collagen content. Cardiac parasitism and inflammation were analyzed with a Zeiss integrating eyepiece with 100 hits (Oberkohen, Germany) at a final magnification of 400X. A total of 3000 hits were evaluated in each section of cardiac tissue. The infection and inflammation indices represent the number of hits covered by amastigote nests and inflammatory cells, respectively.

Flow Cytometry

Flow cytometry was performed as previously described [19], with modifications. Briefly, animals were first euthanized under CO_2 anesthesia. Spleens were removed, injected with Liberase CI (0.45 mg/mL, Roche Applied Sciences, Indianapolis, IN), placed in serum-free RPMI 1640 (Invitrogen, Carlsbad, CA), quickly vortexed and then incubated at 37°C for 30

NIH-PA Author Manuscript

NIH-PA Author Manuscript

NIH-PA Author Manuscript

minutes. Spleen single cell suspensions were prepared by passing tissue through a 40-μm nylon cell strainer in PBS containing 2% FBS (Hyclone, Thermo Scientific, Waltham, MA) and EDTA. 4-5 hearts were pooled and minced in Liberase CI (0.45 mg/mL), quickly vortexed, and incubated at 37°C for 30 minutes. The cells were centrifuged in 35% Percoll (Amersham-Pharmacia Biotech, Piscataway, NJ) for 15 min at 700 g. Spleen and heart suspensions were hemolyzed in ACK buffer (Lonza BioWhittaker, Walkersville, MD).

A total of 10^6 freshly isolated cells were analyzed immediately *ex vivo* for surface marker expression or apoptosis/necrosis markers (Annexin V/PI; Annexin V Apoptosis Detection kit conjugated to FITC, eBioscience, San Diego, CA), or after being cultured for 6 h with either medium alone or with plate-bound anti-CD3 (3 μg/ml) for intracellular cytokine expression. During the last 3 h of culture, Brefeldin A and Monensin (1 μg/ml each) (BD Pharmingen, San Jose, CA) were added for intracellular cytokine staining. Before adding antibodies, cells were washed in PBS and incubated for 30 minutes with an amine-reactive fluorescent dye to exclude dead cells (LIVE/DEAD Fixable Violet Dead Cell Stain Kit, Invitrogen). The following labeled rat or hamster anti-mouse mAbs were used: anti-TCR β-Alexa fluor 700 (clone H57-597), anti-CD8-APC Alexa fluor 750 (clone 53-6.7), anti-Gr-1-PECy5 (clone RB6-8C5), all from eBioscience (San Diego, CA); anti-CD11b-FITC (clone M1/70) and anti-I-A/I-E-biotin (clone 2G9), from BD Pharmingen; and anti-CD4-Pacific orange (clone RM4-5), from Caltag-Invitrogen (Carlsbad, CA). Cell suspensions were then fixed and permeabilized according to the manufacturer's instructions (Fix/Perm kit; BD Pharmingen). To analyze activation markers, the cell suspensions were stained with the following labeled rat anti-mouse mAbs: anti-CD44-Pacific Blue (clone IM7, BioLegend, San Diego, CA) and anti-CD62L-PECy7 (clone MEL-14), from eBioscience (San Diego, CA). Intracellular staining was performed using the following labeled rat or hamster anti-mouse mAbs: anti-IL-10-PE (clone JES5-16E3) and anti-IL-17A-PerCP-Cy5.5 (clone TC11-18H10), from BD Pharmingen; anti-IFN-γ-PECy7 (clone XMG1.2), anti-TNF-α Pacific blue (clone MP6-XT22), and anti-Foxp3-FITC (clone FJK-16S), from eBioscience. To analyze cell proliferation, cell suspensions were stained with mouse anti-human Ki-67-PE (clone B56, BD Pharmingen). Quantum dot 605-conjugated streptavidin (Invitrogen, Carlsbad, CA) was added during intracellular staining to bind anti-I-A/I-E-biotin. Data were collected using an LSR II (BD Immunocytometry Systems) with Diva software (BD Biosciences) and analyzed with FlowJo software (Tree Star).

Adoptive Transfer

T cells were pooled from spleens and lymph nodes of 5 naive WT or 5 IL-10 KO mice by negative selection (Pan T Cell Isolation Kit, Miltenyi Biotec). $CD3^+$ T cells were further purified with PE-labeled anti-CD3e (145-2C11, BD Biosciences) by cell sorting using a FACSAria instrument (BD Biosciences). A total of 2×10^6 FACS-purified $CD3^+$ T cells (>98% pure) from WT or IL-10 KO mice were injected i.v. into RAG-1-deficient mice, which were then infected 24 hours later with *T. cruzi* and analyzed for parasitemia and mortality.

Statistical Analyses

Results are shown as means ± SEM. Differences between groups were compared using the Students *t* test (two sets of data) or one-way ANOVA (three or more sets of data), followed by the Student-Newman-Keuls post hoc test. Survival curves were analyzed using the Logrank test. Differences were considered significant at $p < 0.05$.

NIH-PA Author Manuscript
NIH-PA Author Manuscript
NIH-PA Author Manuscript

Results

C57BL/6J mice, but not C3H/HeSnJ mice, control parasitism and survive after infection with *T. cruzi*

During experiments designed to study immunoregulation in the acute phase of *T. cruzi* (Colombiana strain)-induced myocarditis using candidate gene knockout mice on the C57BL/6J background, we found that acute mortality in wild type mice was very low and myocarditis was mild to moderate. This outcome differs from other reports using this strain of *T. cruzi* with C57BL/6 mice [20, 21]. In contrast, during experiments designed to study immunoregulation of the chronic phase of *T. cruzi* (Colombiana strain)-induced cardiomyopathy using C3H/HeSnJ mice, 100% of animals died by 40 days p.i. and myocarditis was severe. This outcome differs from other reports using this strain of *T. cruzi* with C3H/He mice [19, 22, 23]. We do not know why these unexpected outcomes occurred, although possibilities include 1) differences in experimental protocol, including gender and inoculum differences; 2) mutations that may have accrued over time in either the parasite or mouse strain; and 3) environmental differences including changes in the microbiome associated with different animal facilities. Whatever the reason, the existence of these two models of disease using the same parasite strain, same inoculum, same sex, and same mouse facility provided an opportunity to evaluate immunoregulatory correlates of resistance versus susceptibility during the acute phase of infection directly and in a systematic manner.

T. cruzi infection of wild type C3H/HeSnJ mice resulted in low levels of parasitemia until day 14 p.i. when it accelerated dramatically, peaking at 2×10^7 parasites/mL of whole blood (Fig. 1A). In contrast, parasitemia in wild type C57BL/6J mice was much lower than in C3H/HeSnJ mice after day 14 p.i., 20-fold less at peak (32 days p.i.), and slowly and progressively declined until by day 78 p.i., when measurements were discontinued, only an occasional parasite could be detected in some animals (Fig. 1A). Consistent with this, survival of infected C57BL/6J mice in the acute phase was 91.7% until at least 210 days after infection, when the experiments were stopped (Fig. 1B, and data not shown).

We also compared parasite burden in the two mouse lines in heart, spleen and liver after infection (Fig. 1C). Consistent with previous reports that the Colombiana strain is myotropic, *T. cruzi* DNA levels were much greater in the hearts from both lines of mice than in either spleen or liver from the corresponding line. However, C3H/HeSnJ parasite load was greater than C57BL/6J parasite load in all three organs. This was particularly striking in the heart, where parasite burden was 160 times greater for C3H/HeSnJ than for C57BL/6J mice on day 30 p.i. (Fig. 1C). This fold-increase was 16 and 30 times greater than those observed in spleen and liver, respectively.

C3H/HeSnJ mice, but not C57BL/6J mice, develop severe myocarditis and cardiac failure in the acute phase of *T. cruzi* infection

Since *T. cruzi* is able to infect many organs and multiple cell types, we next performed comprehensive anatomic and histopathologic analysis to determine the extent of disease and the proximate cause of death. All C3H/HeSnJ mice examined were either found dead or were euthanized after fulfilling protocol criteria for euthanasia at 28-31 days p.i. C57BL/6J mice were euthanized on day 32 p.i. in good clinical condition. Seven out of 10 C3H/HeSnJ mice examined had pleural effusions secondary to cardiac failure caused by severe myocarditis, which appeared to be the cause of death. The three mice that did not have pleural effusion still had severe myocarditis. Histopathologic analysis showed that the heart (Table I, Fig. 2) and skeletal muscle (data not shown) were the most differentially affected organs in C3H/HeSnJ versus C57BL/6J mice. In addition to severe myocarditis and moderate fibrosis (Fig. 2), the hearts of infected C3H/HeSnJ mice had moderate to severe

NIH-PA Author Manuscript

NIH-PA Author Manuscript

NIH-PA Author Manuscript

multifocal necrosis, multifocal mineralization and numerous amastigote pseudocysts (Table I; Fig. 2). Eight out of ten animals analyzed had endocardial thrombi in the right atrium and/or right ventricle. In contrast, infected C57BL/6J mice had only mild to moderate myocarditis and mild fibrosis, without signs of cardiac necrosis or mineralization and very few amastigote pseudocysts (Table I; Fig. 2). Myocarditis was primarily lymphocytic in both C3H/HeSnJ and C57BL/6J mice, but PMNs were also found in C3H/HeSnJ hearts in association with thrombi (data not shown). In the spleen, both C3H/HeSnJ and C57BL/6J mice had moderate extramedullary hematopoiesis and moderate lymphoid hyperplasia. The livers of both lines of mice had mild extramedullary hematopoiesis. Infected C3H/HeSnJ mice had mild-moderate inflammatory cell infiltrates in all other organs where parasites were detected (brain, spinal cord, brown fat, lung and esophagus); kidney, adrenal gland, thyroid and pancreas lacked both cellular infiltrates and detectable parasites by light microscopy. At the cellular level, parasites were detected in C3H/HeSnJ mice in cardiac myocytes, skeletal muscle myofibers and brown fat adipocytes in 100% of mice examined (n = 9 or 10); in lung myocytes from 6 of 10 mice examined; in brain neurons and glial cells from 3 of 6 mice examined; in spinal cord inflammatory cells and glial cells from 4 of 9 mice examined; and in esophageal myocytes from 3 of 10 mice examined.

Myocardial infiltrates after *T. cruzi* infection have a higher frequency of $Gr1^{hi}CD11b^{+}TCR^{-}$ cells, but a lower frequency of $CD8^{+}$ T cells in C3H/HeSnJ mice compared to C57BL/6J mice

Since C57BL/6J mice appeared to mount a clinically effective and appropriate response to the pathogen, whereas C3H/HeSnJ mice responded ineffectively, we next tested whether this difference in susceptibility could be linked to MHC haplotype, as previously suggested [24]. C3H/HeSnJ mice are H-2k, whereas C57BL/6J mice are H-2b. When we infected C3.SW/SnJ mice, which are C3H/HeSnJ animals that carry MHC haplotype H-2b (the same as C57BL/6J), parasitemia remained uncontrolled and mortality was still 100% (data not shown).

Therefore we next investigated the local immune responses in the heart to identify specific differences at the cellular and molecular level that might contribute to opposite outcomes in these mice. First we isolated leukocytes from hearts for flow cytometric analysis. In both uninfected C57BL/6J mice and uninfected C3H/HeSnJ mice, very few leukocytes were detectable in the heart by either histopathologic examination (data not shown) or by FACS analysis (data not shown). After infection, leukocytes accumulated in greater numbers in C3H/HeSnJ mice relative to C57BL/6J mice, and the distribution of subsets was different. In particular, the frequency of $CD8^{+}TCR\beta^{+}$ T cells was significantly higher in C57BL/6J than in C3H/HeSnJ mice (Fig. 3). Conversely, the frequency of $Gr1^{hi}CD11b^{+}TCR\beta^{-}$ cells, which contains neutrophils, was significantly lower in C57BL/6J than in C3H/HeSnJ mice (Fig. 3). There was no significant difference in the two lines in the frequency of $CD4^{+}TCR\beta^{+}$ T cells, or monocyte/macrophages ($Gr1^{int/-}CD11b^{+}TCR\beta^{-}$ cells) in the heart (Fig. 3). The frequency of $Foxp3^{+}CD4^{+}$ Tregs was also similar in the heart (0.67 ± 0.02 vs $1.23 \pm 0.41\%$ for C57BL/6J and C3H/HeSnJ mice, respectively). Regarding potential mechanisms, the frequency of $Gr1^{hi}CD11b^{+}TCR\beta^{-}$ cells in the spleen before infection was lower in C57BL/6J than in C3H/HeSnJ mice ($0.6 \pm 0.1\%$ vs $1.9 \pm 0.4\%$, $p=0.006$), perhaps accounting in part for the reduced $Gr1^{hi}CD11b^{+}TCR\beta^{-}$ cell frequency found in infected C57BL/6J hearts relative to C3H/HeSnJ hearts (Suppl. Fig. 1A). No statistically significant difference was found in the spleen in the frequency of any other cell type analyzed in the two strains before infection: CD8+ T cells ($32.3 \pm 2.4\%$ vs $27.5 \pm 1.9\%$), CD4+ T cells (51.6 ± 7.6 vs $61.2 \pm 4.1\%$), monocyte/macrophages ($9.1 \pm 2.0\%$ vs $7.9 \pm 0.7\%$), and Tregs (5.4 ± 0.7 vs $6.1 \pm 0.4\%$) for C57BL/6J and C3H/HeSnJ mice, respectively (Suppl. Fig. 1A).

NIH-PA Author Manuscript

NIH-PA Author Manuscript

NIH-PA Author Manuscript

As in the heart, the spleens of infected C57BL/6J mice contained a higher frequency of $CD8^+TCR\beta^+$ cells than spleens from infected C3H/HeSnJ mice (45.5 ± 7.8% vs 28.9 ± 2.3%; p=0.002) (Suppl. Fig. 1A). The frequency of the splenic $CD4^+TCR\beta^+$ population was slightly lower in infected C57BL/6J than infected C3H/HeSnJ mice (30.1 ± 4.0% vs 36.6 ± 3.0%; p=0.02). There was no significant difference between the two strains in the frequency of splenic monocyte/macrophages and PMNs after infection (Suppl. Fig.1A).

T. cruzi induces differential polarization of immunoregulatory cytokine and chemokine gene expression in C57BL/6J versus C3H/HeSnJ mice

To search for molecular candidates that might control outcome after *T. cruzi* infection of C57BL/6J and C3H/HeSnJ mice, we performed a survey of immunoregulatory cytokines and chemokines, effector enzymes and transcription factors, using RNA isolated from the heart 30 days after infection. Of 44 factors tested, infection with *T. cruzi* induced expression by at least 2-fold for 39 in C57BL/6J mice and for all 44 in C3H/HeSnJ mice (Table II). Genes that were expressed at least 5-fold higher in infected C3H/HeSnJ heart relative to infected C57BL/6J heart included those encoding the CXC chemokines Cxcl2, Cxcl9 and Cxcl11; the chemokine receptors Cxcr3, Ccr1, Ccr3, Ccr4 and Ccr6; the cytokines IL-13 and IL-17A; and the effector enzymes Nitric Oxide Synthase-2 (NOS-2) and Arginase-1 (ARG-1). After infection we found strong induction in the hearts of both lines of mice for genes encoding Ccl4 and Ccl5 (the ligands for Ccr5, and Ccr1, Ccr3 and Ccr5 respectively), and IL-12 p40, however the differences between strains for each gene were only ~2-fold. The only factor tested that was strongly overexpressed after infection (8.7-fold) in C57BL/6J heart relative to C3H/HeSnJ heart was IL-10 (Table II).

Myocardial infiltrates after *T. cruzi* infection have a higher frequency of $IL\text{-}10^+CD4^+$ and $IL\text{-}10^+CD8^+$ effector T cell subsets in C57BL/6J mice compared to C3H/HeSnJ mice

We next defined *T. cruzi* induction of IL-10 and other major immunoregulatory cytokine at the protein and cell level by FACS analysis of leukocytes that accumulated in the heart 28-30 days p.i. When leukocytes isolated from either heart or spleen of *T. cruzi*-infected mice were stimulated with either culture medium or *T. cruzi* lysate antigen, no intracellular cytokine production was detectable. However, after stimulation with anti-CD3, we were able to detect $IFN\gamma^+$, $IL\text{-}10^+$ and $TNF\alpha^+$, but not $IL\text{-}17^+$ cells, among both the $CD4^+$ and $CD8^+$ subsets of T cells isolated from infected hearts of both C57BL/6J and C3H/HeSnJ mice (Fig. 4). No $IL\text{-}10^+Gr\text{-}1^{int/-}CD11b^+IA^+TCR\beta^-$ myeloid cells were identified. Also, we were not able to detect these four intracellular cytokines in splenocytes isolated from uninfected mice from either strain after stimulation with anti-CD3 (data not shown). Consistent with increased gene expression for Cxcr3 and IFNγ in infected C3H/HeSnJ mice relative to infected C57BL/6J mice, we observed a higher frequency of $IFN\gamma^+CD4^+$ and $IFN\gamma^+CD8^+$ T cells in the hearts of infected C3H/HeSnJ mice relative to infected C57BL/6J mice, although the differences were less than 2-fold. There were also differences in the frequency of TNFα-producing $CD4^+$ and $CD8^+$ T cells and IL-10-producing $CD4^+$ T cells after infection between C57BL/6J and C3H/HeSnJ mice, but again the differences were at most ~2-fold. In contrast, the frequency of IL-10-producing $CD8^+$ T cells was much greater, approximately 10-fold, in infected hearts from C57BL/6J mice compared with hearts from infected C3H/HeSnJ mice (Fig. 4C).

Analysis of double-cytokine producing cells in the heart upon *T. cruzi* infection revealed additional large differences between the two strains related to IL-10. None of the $IL\text{-}10^+CD4^+$ or $IL\text{-}10^+CD8^+$ T cells in either infected C57BL/6J or infected C3H/HeSnJ hearts was also producing TNFα (data not shown). Yet, in infected C57BL/6J hearts most (~99%) of the $IL\text{-}10^+CD4^+$ and $IL\text{-}10^+CD8^+$ T cells were also producing IFNγ (Fig. 4B-C). In striking contrast, in infected C3H/HeSnJ hearts there were almost no $IL\text{-}10^+CD8^+$ T cells

NIH-PA Author Manuscript

NIH-PA Author Manuscript

NIH-PA Author Manuscript

(~1%) (Fig. 4B-C) and very few IL-10$^+$CD4$^+$ T cells (6%); most of the IL-10$^+$CD4$^+$ T cells were also producing IFNγ (Fig. 4B-C). All IFNγ$^+$CD8$^+$ T cells from infected C3H/HeSnJ hearts failed to express IL-10, and thus appeared to have a classic Th1 immunophenotype (Fig. 4B-C), whereas in infected C57BL/6J hearts 35% of the IFNγ$^+$CD8$^+$ T cells were also positive for IL-10 (Fig. 4B-C); infected hearts from neither strain of mice contained IL-10$^+$IFNγ$^-$CD8$^+$ T cells (Fig. 4B-C).

Regarding TNFα, the frequency of IFNγ$^+$TNFα$^+$CD8$^+$ T cells was similar in infected C57BL/6J and C3H/HeSnJ hearts (Fig. 4B-C), and the frequency of IFNγ$^+$TNFα$^+$CD4$^+$ T cells was only 2-fold greater in infected C3H/HeSnJ than in infected C57BL/6J hearts (Fig. 4B-C). Very few TNFα$^+$IFNγ$^-$ cells were detectable in either the CD4$^+$ or CD8$^+$ T cell population in either strain of infected mice (Fig. 4B-C). In the spleen of infected C57BL/6J mice, in both the CD4$^+$ and CD8$^+$ TCRβ$^+$ populations, single positive cells for IFNγ and TNFα and double positive cells for IFNγ/TNFα were increased compared to infected C3H/HeSnJ mouse spleen (Suppl. Fig. 1B and C). Thus the level of IL-10 production in the heart by infiltrating CD8+ T cells stood out as a major correlate of susceptibility in C3H/HeSnJ versus C57BL/6J mice infected with *T. cruzi*.

Since IL-10 is an important regulator of cytokine synthesis by APCs, it is possible that under conditions where it is present in low amounts, as in infected C3H/HeSnJ mice, T cells become overwhelmingly activated and die. To test this possibility, we analyzed activation, proliferation and apoptosis markers in T cell populations. A slightly higher percentage of activated CD8$^+$ T cells (CD62L^{lo}CD44^{hi}) was detected in infected hearts of C57BL/6J mice compared to infected C3H/HeSnJ mice (Suppl. Fig. 2A). No difference was detected in the expression of the proliferation marker Ki-67 in CD4$^+$ and CD8$^+$ T cell populations isolated from infected hearts in both strains (Suppl. Fig. 2B). Finally, staining with Annexin V and propidium iodide (PI) for measurement of apoptotic and necrotic cells, respectively, revealed a higher percentage of CD4$^+$, but not CD8$^+$, T cells undergoing cell death in hearts from infected C57BL/6J mice than from infected C3H/HeSnJ mice (Suppl. Fig. 2C and D). Thus, the data do not support massive overactivation and death of T cells in C3H/HeSnJ mice as a likely mechanism for failure to control the parasite in this strain.

A particularly striking finding from this analysis is that in the infected heart the frequency of IL-10$^+$IFNγ$^-$ cells was higher in C57BL/6J mice than in C3H/HeSnJ mice in both the CD8$^+$ and CD4$^+$ T cell populations (Fig. 4B-C), whereas the frequency of IFNγ$^+$IL-10$^-$ cells was higher in C3H/HeSnJ mice than in C57BL/6J mice in both CD8$^+$ and CD4$^+$ T cell populations (Fig. 4B-C). Together these observations suggested that IL-10 coming from both IFNγ/IL-10 double producer and IL-10 single producer T lymphocytes might prevent the intense inflammatory response and parasitemia observed in *T. cruzi*-infected C3H/HeSnJ strain.

T. cruzi infection in a highly resistant C57BL/6J model is uniformly fatal in the absence of IL-10

To test the functional importance of IL-10 in *T.cruzi*-infected mice, we infected IL-10-deficient mice on the C57BL/6J background. As expected, parasitemia in wild type control mice peaked at day 30 and was cleared by day 50 (Fig. 5A). In contrast, IL-10$^{-/-}$ mice on the C57BL/6J background failed to clear parasitemia, which increased linearly until death of all animals, just as we had observed with infected wild type C3H/HeSnJ mice (Fig 5A). Death occurred between 20-42 days p.i., whereas 95% of wild type control mice survived through day 90, when the experiment was terminated (Fig. 5B). Interestingly, IL-10 knockout mice began to die before the WT and KO parasitemia curves began to diverge. Similar to what we had observed with low IL-10-producing C3H/HeSnJ mice after infection, hearts from infected IL-10 KO mice had significantly higher levels of parasite DNA (Fig

NIH-PA Author Manuscript

NIH-PA Author Manuscript

NIH-PA Author Manuscript

5C), more amastigote nests (Fig. 5D) and more intense myocarditis (Fig. 5D, E) when compared to infected WT C57BL/6J mice.

IL-10 deficiency skews the distribution, proliferation and survival of T cells in the hearts of *T. cruzi*-infected mice

We next compared T cell activation, proliferation, apoptosis and necrosis in the hearts of IL-10 KO and control mice. As we had observed for C3H/HeSnJ mice (Fig. 3C), after infection we observed a reduced frequency of $CD8^+$ T cells in hearts of IL-10 KO mice compared to C57BL/6J WT mice (Fig. 6A). However, unlike infected C3H/HeSnJ (Fig. 3C) and C57BL/6J mice, infected IL-10 KO mice had a predominance of $CD4^+$ T cells in the myocardium (Fig. 6A). In addition, the frequency of $Foxp3^+$ $CD4^+$ Treg cells was significantly reduced in hearts isolated from infected IL-10-deficient mice as compared to infected control mice (Fig. 6B). We also found a slightly decreased percentage of $CD8^+$ T cells that were Ki-67^+ in the hearts of infected IL-10 knockout mice (Fig. 6C), suggesting a lower proliferative capacity compared to controls. Regarding activation, however, no difference between the two infected strains was identified in CD44 and CD62L expression by cardiac $CD4^+$ or $CD8^+$ T cells. Of note, double staining by both Annexin V and PI was increased in both $CD4^+$ and $CD8^+$ T cells isolated from infected IL-10 KO hearts as compared to controls (Fig. 6E), but single-stained Annexin V+ cells were similar in frequency (Fig. 6F), suggesting that a higher percentage of the cells is undergoing late apoptosis or necrosis in infected IL-10 KO mice.

In the spleen, we observed an inverted CD4/CD8 ratio in infected IL-10 ko mice compared to controls, with the frequency of $CD4^+$ T cells significantly increased compared to infected WT mice (Suppl. Fig. 3A). In addition, splenic $CD4^+$ T cells from infected IL-10 ko mice had a slightly increased percentage of activated cells ($CD44^{hi}CD62L^{lo}$) compared to infected WT mice (Suppl. Fig. 3A). No difference was observed in expression of the proliferation marker Ki-67 (Suppl. Fig. 3A). However, in the $CD8^+$ T cell population (Suppl. Fig. 3B), we found a decreased percentage of activated and proliferating cells ($CD44^{hi}CD62L^{lo}$ and Ki-67^+, respectively) (Suppl. Fig. 3B). With regard to cell death, there was an increased frequency of both $CD4^+$ and $CD8^+$ T cells undergoing apoptosis in infected WT mice as compared to infected IL-10 KO mice (Suppl. Fig. 3A and B). However, an increased percentage of $CD4^+$ $AnnexinV^+$ PI^+ cells was observed in IL-10-deficient mice (Suppl. Fig. 3A), suggesting that an increased rate of late apoptosis/necrosis was occurring in the spleens of these mice.

Adoptive transfer of T cells from wild type mice, but not from IL-10 knockout mice, prolongs survival of *T. cruzi*-infected RAG-1 deficient mice

We hypothesized that the source of IL-10 protecting mice from fatal *T. cruzi* infection in C57BL/6J mice was the T cell. To test this, we transferred sorted $CD3^+$ T cells isolated from either WT or IL-10 KO mice to *T. cruzi*-infected RAG-1-deficient mice, which produce no mature T or B cells and have been previously shown to be extremely susceptible to *T. cruzi* infection [13]. Confirming this, we found that 100% of RAG-1-deficient mice succumbed to infection by day 24 p.i., with parasitemia increasing linearly with time, reaching levels as high as 3.5×10^7 parasites/mL at death (Fig. 7). Consistent with our hypothesis, transfer of $CD3^+$ T cells isolated from naïve WT mice into infected RAG-1 KO mice significantly prolonged survival, although not to wild type levels, with the final mouse dying on day 37 p.i. ($p<0.0001$, Fig. 7). Moreover, in adoptively transferred mice parasitemia appeared to be well-controlled until day 23 p.i., after which it increased linearly until death of the animals, reaching levels as high as 4.2×10^6 parasites/mL (Fig. 7). In contrast, $CD3^+$ T cells isolated from naïve IL-10 KO mice were not protective when injected into infected RAG-1 KO mice.

NIH-PA Author Manuscript

NIH-PA Author Manuscript

NIH-PA Author Manuscript

On the contrary, they accelerated mortality slightly, with 100% of mice dying on either day 19 or 20 p.i (p=0.0008, Fig. 7B).

Discussion

In the present study, we have demonstrated that IL-10 is a strong protective factor against fatal acute myocarditis in a mouse model of *T. cruzi* infection. Our results are consistent with previous reports in which genetic inactivation or immunologic neutralization of IL-10 increased mortality and acute myocarditis in mouse models of *T. cruzi* infection [12-15], and extend those reports in four important ways: 1) by identifying the T cell as a critical source of protective IL-10 through adoptive transfer studies; 2) by delineating the precise immunophenotypes of IL-10$^+$ T cell subsets accumulating in the hearts of infected mice; 3) by showing that IL-10 deficiency results not only in exaggerated immunopathology in the hearts of infected mice, but also in loss of parasite control; and 4) by showing that *T. cruzi* infection of IL-10 KO C57Bl/6J mice phenocopies infection in wild type parasite-susceptible C3H/HeSnJ mice, in which IL-10 induction by the parasite is weak.

With regard to finding #3, earlier reports had also described exaggerated immunopathology in *T. cruzi*-infected IL-10 knockout mice, but in contrast to our study, this occurred in the face of reduced parasitemia levels [12-15]. The discrepancy may be due to the fact that parasitemia was simply not measured at the relevant time points in the previous studies. In fact, we also found reduced parasitemia in IL-10 knockout mice at early stages post-infection, when parasitemia is also quite low in wild type mice (day 14 in Figure 1 and 5). However, the major point is that there is a critical timepoint, 14-21 days post-infection in mice, beyond which there is a loss of control and parasitemia increases inexorably with time.

In the hearts of infected parasite-resistant C57BL/6J mice, we found that both CD4$^+$ and CD8$^+$ T cells express IL-10, and, consistent with a functional role, that transfer of CD3$^+$ T cells from WT but not from IL-10 KO mice delayed mortality in susceptible RAG-1 KO mice. Additional work will be needed to precisely define whether the relevant CD3$^+$ T cell source of IL-10 in the model is CD4$^+$, CD8$^+$ or both. Moreover, since rescue of infected RAG-1 knockout mice with WT CD3$^+$ T cell transfer was incomplete, other IL-10-producing leukocytes outside the T cell lineage may also contribute to protection in the model. Interestingly, the effect on parasitemia was also intermediate in RAG-1-deficient mice transferred with WT CD3$^+$ T cells, which suggests that either a threshold has been crossed or else that other factors collaborate with parasitemia level to determine the mortality rate in the model. The role of CD8$^+$ T cells in *T. cruzi* infection is likely to be complex. Although they are thought to contribute to immunopathology in patients with chronic chagasic cardiomyopathy [9, 25, 26], in mice they are highly protective during acute infection. In both CD8- and CD4-deficient animals, parasitemia is exacerbated, showing that CD4$^+$ and CD8$^+$ T cells are crucial for parasite control [27]. CD8-deficient mice have been reported to die earlier than CD4-deficient mice [27].

A complete description of how IL-10 limits parasitemia and immunopathology in the model is not yet available, and previous work in this area has provided some conflicting results. Thus, in vitro IL-10 has been reported to inhibit IFNγ-dependent [28, 29] but to promote LPS-dependent [30] elimination of the parasite. *In vivo*, immunopathology has been reported to result from dysregulated type 1 immune responses [14] resulting in a state of systemic toxic shock mediated by TNF-α [15]. Alternatively, IL-10 deficiency could result in a state of T cell hyperactivation, leading to anergy and/or increased cell death. The picture in the heart of IL-10 KO mice is not fully consistent with this, however, since we found an increased percentage of T cells undergoing late apoptosis/necrosis, but a reduced frequency

NIH-PA Author Manuscript

NIH-PA Author Manuscript

NIH-PA Author Manuscript

of total and proliferating $CD8^+$ T cells, and a low frequency of Tregs. In infected C3H/HeSnJ mice we found a decreased percentage of total and activated $CD8^+$ T cells in the heart.

Another possible mechanism is that T cell IL-10 could modulate outcome by regulating leukocyte chemotactic signaling in the heart. However, in a small survey of relevant chemotactic receptors we found no difference by FACS in expression of Ccr1, Ccr5 or Cxcr3 on $IFN\gamma^+/IL\text{-}10^-$ or $IFN\gamma^+/IL\text{-}10^+$ T cells from infected hearts (data not shown). In a preliminary survey of chemokine expression in the heart, we found that infected IL-10 KO mice had higher levels of Cxcl2 than infected wild type mice, while levels of Ccl2, Cxcl9 and Cxcl11, already demonstrated to be protective against *T. cruzi*, were statistically significantly greater in WT mice than in IL-10 KO mice (Suppl. Fig. 4). Additional work will be needed to define the functional role of chemokines in IL-10-mediated protection in the model. With regard to Tregs, although there was no difference in the frequency between C3H/HeSnJ and C57BL/6J, the percentage was reduced in hearts of IL-10 KO mice. However, previous studies have indicated that Tregs, which also produce IL-10, play a minor role in the control of *T. cruzi* [31, 32].

Almost all $IL\text{-}10^+$ cells within both CD4 and CD8 positive T cell subpopulations also expressed IFNγ. The importance of the $IL\text{-}10^+IFN\gamma^+$ double-producing $CD8^+$ T cell subset was also suggested by the almost complete and selective absence of this subset in hearts from parasite-susceptible C3H/HeSnJ mice. In contrast, $IL\text{-}10^+CD4^+$ T cells were only modestly decreased in hearts from infected C3H/HeSnJ mice. $IFN\gamma^+IL\text{-}10^+$ conventional $T\text{-}bet^+Foxp3^-$Th1 cells were first described in 2007 in the context of a mouse model of *Toxoplasma gondii* infection [33] and subsequently in the context of *Influenza* infection [34]. In *T. gondii* infection, these cells were predominantly $CD4^+$ T cells, whereas in the *Influenza* model they were predominantly $CD8^+$ T cells. The $IFN\gamma^+IL\text{-}10^+$ T cell population was shown to be crucial for immunoregulation of the response developed during infection with both pathogens [33, 34], and the $IL\text{-}10^+IFN\gamma^+$ population displayed potent effector function against *T. gondii* [33]. It is well known that IFNγ deficient mice have dramatic parasitism and mortality when infected with *T. cruzi* [35]. However, our results show that C3H/HeSnJ mice are able to produce high levels of IFNγ in the heart, even more than in infected C57BL/6J mice, at least after 30 days of infection. Thus this cytokine may be necessary for protection, but it is not sufficient. With regard to other functionally important cytokines, TNFα has been shown to synergize with IFNγ for optimal nitric oxide (NO) production to eliminate intracellular parasitism in macrophages [29]. On the other hand, TNFα has been suggested to promote heart tissue damage during *T. cruzi* infection [36]. Our data show that the absolute levels of IFNγ and TNFα poorly correlate with outcome, since C3H/HeSnJ mice have a higher frequency of IFNγ/TNFα double-producing T cells in the heart. So, higher amounts of TNFα could be a factor that drives immunopathology in C3H/HeSnJ mice, but this does not explain why parasitism is not controlled.

Although our results clearly establish a protective role for IL-10 in *T. cruzi*-infected C57BL/6J mice, the precise contribution of low IL-10 production to susceptibility in infected C3H/HeSnJ mice and the molecular basis for its deficiency were not addressed directly by our study. Next steps include mapping the gene(s) responsible for the susceptibility phenotype difference between the two strains of mice. It has been known for years that the phenotype of the F1 progeny of C3H/HeJ × C57BL/6J, as well as other H-2k × H-2b matings, is complex. F1 mice have been reported to have low parasitemia, with mortality differing by gender: females survive infection > 120 days, whereas males die later than susceptible parents but earlier than resistant parents [24]. Thus, the genes responsible for low parasitemia appear to be expressed in a dominant manner (Wrightsman et al., 1982). However, IL-10 was not measured in these previous studies. A plausible mechanism for the

NIH-PA Author Manuscript

NIH-PA Author Manuscript

NIH-PA Author Manuscript

IL-10 defect in infected C3H/HeSnJ mice is defective innate immune recognition, since Toll-like Receptors (TLRs) and Nod-like receptors (NLRs) are important for host resistance against *T. cruzi* infection [37] and induce IL-10 production. Stimulation of innate immune cells by *T. cruzi*-derived GPI anchors and DNA has been reported to activate TLR2, 4, 7 and 9 [38-41], leading to production of parasiticidal agents, optimal activation of APCs and proper activation of adaptive immune responses. With regard specifically to TLR4, we observed no difference in parasitemia or mortality for the Jackson C3H/HeJ line #659, which has a spontaneous mutation inactivating the TLR4 gene, and the Jackson C3H/HeSnJ line #661, which has a wild type TLR4 gene (data not shown). In a related report, Oliveira et al. have shown that C3H/HeJ and TLR4 KO mice are slightly more susceptible to infection with the reticulotropic Y strain of *T. cruzi* than C3H/HeN mice [39]. The difference relative to our experiment could relate to differences in the source of the mice and/or the precise parasite strain that was used, but in any case was not large. Additional work will be needed to define the role of other pattern recognition receptors in IL-10 deficiency in the model.

In conclusion, we show that C3H/HeSnJ mice provide a model of acute fulminant myocarditis after *T. cruzi* (Colombiana strain) infection, the result of an exuberant but ineffective immune response against the pathogen, whereas C57BL/6J mice provide a model of mild acute cardiac disease, the result of a more effective immune response. IL-10 strongly correlated with outcome and we directly demonstrated its functional importance in the model in C57Bl/6J mice. T cells constitute a source of protective IL-10, and both $CD4^+$ and $CD8^+$ subsets in the hearts of infected mice produce it, however other T cell-independent sources appear to exist and remain to be defined. Almost all of the $IL\text{-}10^+$ T cells in the heart also produce IFNγ, however the precise functional role of these cells remains to be delineated. Based on all these considerations, we hypothesize that upon *T. cruzi* (Colombiana strain) infection, IL-10 deficiency abrogates expansion of a cardioprotective $IFN\gamma^+IL\text{-}10^+CD8^+$ T cell population in C57Bl/6J mice in this model. Why infected C3H/HeSnJ mice are selectively unable to generate this population of cells in the heart is an important question for future research. Together, our results support a role for IL-10 as a potentially beneficial immunodulatory agent in *T. cruzi* infection.

Supplementary Material

Refer to Web version on PubMed Central for supplementary material.

Acknowledgments

We are grateful to Dr. Fuyuki Tokumasu and Dr. James Dvorak (Laboratory of Malaria and Vector Research, NIAID/NIH) for the kind donation of the Colombiana strain of *T. cruzi*, to Tom Moyer, from the NIAID Research Technologies Branch, for performing the cell sorting, and to Rick Dreyfuss, from the NIH Division of Medical Arts, for preparing photomicrographs. We are also grateful to Dragana Jankovic (Laboratory of Parasitic Diseases, NIAID/NIH) for valuable ideas and discussion.

Grant Support

This work was supported by the Division of Intramural Research, NIAID, NIH, Department of Health and Human Services, USA.

References

[1]. Schofield CJ, Jannin J, Salvatella R. The future of Chagas disease control. Trends in Parsitol. 2006; 22:583–588.

[2]. Urbina JA. Specific chemotherapy of Chagas' disease: relevance, current limitations and new approaches. Acta Trop. 2010; 115:55–68. [PubMed: 19900395]

NIH-PA Author Manuscript

NIH-PA Author Manuscript

NIH-PA Author Manuscript

[3]. Rocha MO, Nunes MC, Ribeiro AL. Morbidity and prognostic factors in chronic chagasic cardiopathy. Mem Inst Oswaldo Cruz. 2009; 104:159–166. [PubMed: 19753471]

[4]. Marin-Neto JA, Cunha-Neto E, Maciel BC, Simões MV. Pathogenesis of chronic Chagas heart disease. Circulation. 2007; 115:1109–1123. [PubMed: 17339569]

[5]. Michailowsky V, Silva NM, Rocha CD, Vieira LQ, Lannes-Vieira J, Gazzinelli RT. Pivotal role of interleukin-12 and interferon-gamma axis in controlling tissue parasitism and inflammation in the heart and central nervous system during *Trypanosoma cruzi* infection. Am J Pathol. 2001; 159:1723–1733. [PubMed: 11696433]

[6]. Hardison JL, Kuziel WA, Manning JE, Lane TE. Chemokine CC receptor 2 is important for acute control of cardiac parasitism but does not contribute to cardiac inflammation after infection with *Trypanosoma cruzi*. J Infect Dis. 2006; 193:1584–1588. [PubMed: 16652288]

[7]. Machado FS, Koyama NS, Carregaro V, Ferreira BR, Milanezi CM, Teixeira MM, Rossi MA, Silva JS. CCR5 plays a critical role in the development of myocarditis and host protection in mice infected with *Trypanosoma cruzi*. J Infect Dis. 2005; 191:627–636. [PubMed: 15655788]

[8]. Hardison JL, Wrightsman RA, Carpenter PM, Lane TE, Manning JE. The chemokines CXCL9 and CXCL10 promote a protective immune response but do not contribute to cardiac inflammation following infection with *Trypanosoma cruzi*. Infect Immun. 2006; 74:125–134. [PubMed: 16368965]

[9]. Reis MM, Higuchi ML, Benvenuti LA, Aiello VD, Gutierrez PS, Bellotti G, Pileggi F. An *in situ* quantitative immunohistochemical study of cytokines and IL-2R+ in chronic human chagasic myocarditis: correlation with the presence of myocardial *Trypanosoma cruzi* antigens. Clin Immunol Immunopathol. 1997; 83:165–172. [PubMed: 9143377]

[10]. Gomes JA, Bahia-Oliveira LM, Rocha MO, Martins-Filho OA, Gazzinelli G, Correa-Oliveira R. Evidence that development of severe cardiomyopathy in human Chagas' disease is due to a Th1-specific immune response. Infect Immun. 2003; 71:1185–1193. [PubMed: 12595431]

[11]. Federici EE, Abelmann WH, Neva FA. Chronic and progressive myocarditis and myositis in C3H mice infected with *Trypanosoma cruzi*. Am J Trop Med Hyg. 1964; 13:272–280. [PubMed: 14125879]

[12]. Reed SG, Brownell CE, Russo DM, Silva JS, Grabstein KH, Morrissey PJ. IL-10 mediates susceptibility to Trypanosoma cruzi infection. J Immunol. 1994; 153:3135–3140. [PubMed: 8089491]

[13]. Abrahamsohn IA, R L. Coffman. Trypanosoma cruzi: IL-10, TNF, IFN-gamma, and IL-12 regulate innate and acquired immunity to infection. Exp Parasitol. 1996; 84:231–244. [PubMed: 8932773]

[14]. Hunter CA, Ellis-Neyes LA, Slifer T, Kanaly S, Grünig G, Fort M, Rennick D, Araujo FG. IL-10 is required to prevent immune hyperactivity during infection with Trypanosoma cruzi. J Immunol. 1997; 158:3311–3316. [PubMed: 9120288]

[15]. Hölscher C, Mohrs M, Dai WJ, Köhler G, Ryffel B, Schaub GA, Mossmann H, Brombacher F. Tumor necrosis factor alpha-mediated toxic shock in Trypanosoma cruzi-infected interleukin 10-deficient mice. Infect Immun. 2000; 68:4075–4083. [PubMed: 10858224]

[16]. Brener Z. Therapeutic activity and criterion of cure on mice experimentally infected with *Trypanosoma cruzi*. Rev. Inst. Med. Trop. São Paulo. 1962; 39:389–396.

[17]. Santiago HC, Feng CG, Bafica A, Roffe E, Arantes RM, Cheever A, Taylor G, Vieira LQ, Aliberti J, Gazzinelli RT, Sher A. Mice deficient in LRG-47 display enhanced susceptibility to *Trypanosoma cruzi* infection associated with defective hemopoiesis and intracellular control of parasite growth. J Immunol. 2005; 175:8165–8172. [PubMed: 16339555]

[18]. Cummings KL, Tarleton RL. Rapid quantitation of *Trypanosoma cruzi* in host tissue by real-time PCR. Mol Biochem Parasitol. 2003; 129:53–59. [PubMed: 12798506]

[19]. Santos PVA, Roffê E, Santiago HC, Torres RA, Marino APMP, Paiva CN, Silva AA, Gazzinelli RT, Lannes-Vieira J. Prevalence of CD8 + T cells in *Trypanosoma cruzi*-elicited myocarditis is associated with acquisition of CD62L low LFA-1 high VLA-4 high activation phenotype and expression of IFN- -inducible adhesion and chemoattractant molecules. Microbes Infect. 2001; 3:971–984. [PubMed: 11580984]

NIH-PA Author Manuscript

NIH-PA Author Manuscript

NIH-PA Author Manuscript

[20]. Talvani A, Ribeiro CS, Aliberti JC, Michailowsky V, Santos PV, Murta SM, Romanha AJ, Almeida IC, Farber J, Lannes-Vieira J, Silva JS, Gazzinelli RT. Kinetics of cytokine gene expression in experimental chagasic cardiomyopathy: tissue parasitism and endogenous IFN-gamma as important determinants of chemokine mRNA expression during infection with Trypanosoma cruzi. Microbes Infect. 2000; 2:851–866. [PubMed: 10962268]

[21]. Michailowsky V, Celes MR, Marino AP, Silva AA, Vieira LQ, Rossi MA, Gazzinelli RT, Lannes-Vieira J, Silva JS. Intercellular adhesion molecule 1 deficiency leads to impaired recruitment of T lymphocytes and enhanced host susceptibility to infection with Trypanosoma cruzi. J Immunol. 2004; 173:463–470. [PubMed: 15210806]

[22]. Silva AA, Roffe E, Marino AP, dos Santos PV, Quirico-Santos T, Paiva CN, Lannes-Vieira J. Chagas' disease encephalitis: intense CD8+ lymphocytic infiltrate is restricted to the acute phase, but is not related to the presence of Trypanosoma cruzi antigens. Clin Immunol. 1999; 92:56–66. [PubMed: 10413653]

[23]. Medeiros GA, Silvério JC, Marino AP, Roffê E, Vieira V, Kroll-Palhares K, Carvalho CE, Silva AA, Teixeira MM, Lannes-Vieira J. Treatment of chronically Trypanosoma cruzi-infected mice with a CCR1/CCR5 antagonist (Met-RANTES) results in amelioration of cardiac tissue damage. Microbes Infect. 2009; 11:264–273. [PubMed: 19100857]

[24]. Wrightsman R, Krassner S, Watson J. Genetic control of responses to Trypanosoma cruzi in mice: multiple genes influencing parasitemia and survival. Infect Immun. 1982; 36:637–644. [PubMed: 6806192]

[25]. Higuchi ML, Gutierrez PS, Aiello VD, Palomino S, Bocchi E, Kalil J, Bellotti G, Pileggi F. Immunohistochemical characterization of infiltrating cells in human chronic chagasic myocarditis: comparison with myocardial rejection process. Virchows Arch A Pathol Anat Histopathol. 1993; 423:157–160. [PubMed: 7901937]

[26]. Reis DD, Jones EM, Tostes S Jr, Lopes ER, Gazzinelli G, Colley DG, McCurley TL. Characterization of inflammatory infiltrates in chronic chagasic myocardial lesions: presence of tumor necrosis factor-alpha+ cells and dominance of granzyme A+, CD8+ lymphocytes. Am J Trop Med Hyg. 1993; 48:637–644. [PubMed: 8517482]

[27]. Rottenberg ME, Bakhiet M, Olsson T, Kristensson K, Mak T, Wigzell H, Orn A. Differential susceptibilities of mice genomically deleted of CD4 and CD8 to infections with Trypanosoma cruzi or Trypanosoma brucei. Infect Immun. 1993; 61:5129–5133. [PubMed: 8225589]

[28]. Silva JS, Morrissey PJ, Grabstein KH, Mohler KM, Anderson D, Reed SG. Interleukin 10 and interferon gamma regulation of experimental Trypanosoma cruzi infection. J Exp Med. 1992; 175:169–174. [PubMed: 1730915]

[29]. Gazzinelli RT, Oswald IP, Hieny S, James SL, Sher A. The microbicidal activity of interferon-gamma-treated macrophages against Trypanosoma cruzi involves an L-arginine-dependent, nitrogen oxide-mediated mechanism inhibitable by interleukin-10 and transforming growth factor-beta. Eur J Immunol. 1992; 22:2501–2506. [PubMed: 1396957]

[30]. Jacobs F, Chaussabel D, Truyens C, Leclerq V, Carlier Y, Goldman M, Vray B. IL-10 up-regulates nitric oxide (NO) synthesis by lipopolysaccharide (LPS)-activated macrophages: improved control of Trypanosoma cruzi infection. Clin Exp Immunol. 1998; 113:59–64. [PubMed: 9697984]

[31]. Kotner J, Tarleton R. Endogenous CD4(+) CD25(+) regulatory T cells have a limited role in the control of Trypanosoma cruzi infection in mice. Infect Immun. 2007; 75:861–869. [PubMed: 17101658]

[32]. Mariano FS, Gutierrez FR, Pavanelli WR, Milanezi CM, Cavassani KA, Moreira AP, Ferreira BR, Cunha FQ, Cardoso CR, Silva JS. The involvement of CD4+CD25+ T cells in the acute phase of Trypanosoma cruzi infection. Microbes Infect. 2008; 10:825–833. [PubMed: 18538611]

[33]. Jankovic D, Kullberg MC, Feng CG, Goldszmid RS, Collazo CM, Wilson M, Wynn TA, Kamanaka M, Flavell RA, Sher A. Conventional T-bet(+)Foxp3(-) Th1 cells are the major source of host-protective regulatory IL-10 during intracellular protozoan infection. J Exp Med. 2007; 204:273–283. [PubMed: 17283209]

[34]. Sun J, Madan R, Karp CL, Braciale TJ. Effector T cells control lung inflammation during acute influenza virus infection by producing IL-10. Nat Med. 2009; 15:277–284. [PubMed: 19234462]

NIH-PA Author Manuscript

NIH-PA Author Manuscript

NIH-PA Author Manuscript

[35]. Hölscher C, Köhler G, Müller U, Mossmann H, Schaub GA, Brombacher F. Defective nitric oxide effector functions lead to extreme susceptibility of Trypanosoma cruzi-infected mice deficient in gamma interferon receptor or inducible nitric oxide synthase. Infect Immun. 1998; 66:1208–1215. [PubMed: 9488415]

[36]. Kroll-Palhares K, Silvério JC, Silva AA, Michailowsky V, Marino AP, Silva NM, Carvalho CM, Pinto LM, Gazzinelli RT, Lannes-Vieira J. TNF/TNFR1 signaling up-regulates CCR5 expression by CD8+ T lymphocytes and promotes heart tissue damage during Trypanosoma cruzi infection: beneficial effects of TNF-alpha blockade. Mem Inst Oswaldo Cruz. 2008; 103:375–385. [PubMed: 18660993]

[37]. Tarleton RL. Immune system recognition of Trypanosoma cruzi. Curr Opin Immunol. 2007; 19:430–434. [PubMed: 17651955]

[38]. Campos MA, Almeida IC, Takeuchi O, Akira S, Valente EP, Procópio DO, Travassos LR, Smith JA, Golenbock DT, Gazzinelli RT. Activation of Toll-like receptor-2 by glycosylphosphatidylinositol anchors from a protozoan parasite. J Immunol. 2001; 167:416–423. [PubMed: 11418678]

[39]. Oliveira AC, Peixoto JR, de Arruda LB, Campos MA, Gazzinelli RT, Golenbock DT, Akira S, Previato JO, Mendonça-Previato L, Nobrega A, Bellio M. Expression of functional TLR4 confers proinflammatory responsiveness to Trypanosoma cruzi glycoinositolphospholipids and higher resistance to infection with T. cruzi. J Immunol. 2004; 173:5688–5696. [PubMed: 15494520]

[40]. Caetano BC, Carmo BB, Melo MB, Cerny A, dos Santos SL, Bartholomeu DC, Golenbock DT, Gazzinelli RT. Requirement of UNC93B1 reveals a critical role for TLR7 in host resistance to primary infection with Trypanosoma cruzi. J Immunol. 2011; 187:1903–1911. [PubMed: 21753151]

[41]. Bafica A, Santiago HC, Goldszmid R, Ropert C, Gazzinelli RT, Sher A. Cutting edge: TLR9 and TLR2 signaling together account for MyD88-dependent control of parasitemia in Trypanosoma cruzi infection. J Immunol. 2006; 177:3515–3519. [PubMed: 16951309]

NIH-PA Author Manuscript
NIH-PA Author Manuscript
NIH-PA Author Manuscript

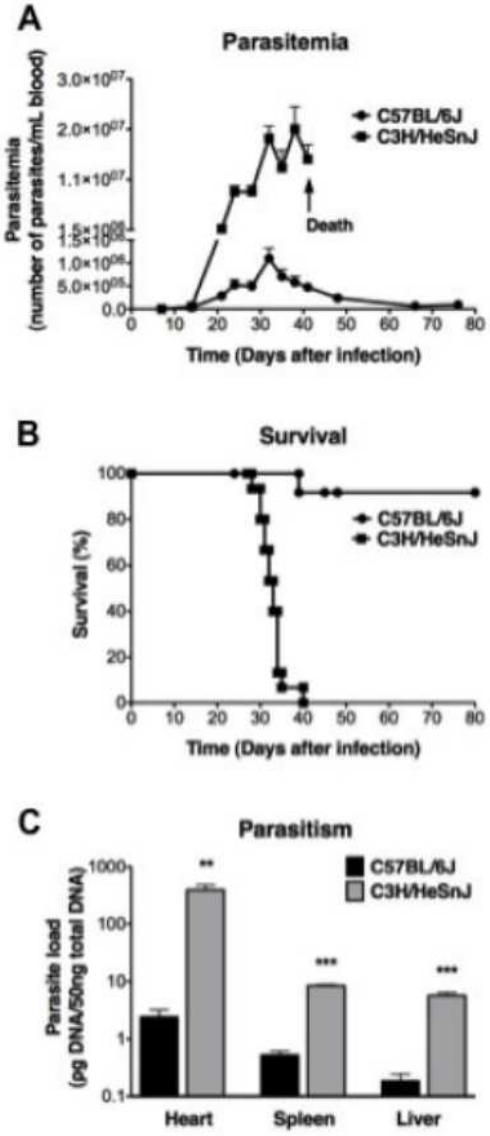

Figure 1. C57BL/6J mice, but not C3H/HeSnJ mice, control parasitism and survive infection with *T. cruzi*

A) Parasitemia. Data are the mean ± SEM from a single experiment (n=15 animals in each group) representative of 3 independent experiments. B) Survival. Data are from the same experiment shown in panel A (n=15 animals per group), representative of 3 independent experiments. $P < 0.0001$ by Logrank test. C) Quantification of *T. cruzi* DNA in tissues of *T. cruzi*-infected mice. Heart, spleen and liver were collected from C3H/HeSnJ and C57BL/6J mice 30 days after infection, and *T. cruzi* burden was quantitated by PCR. Results are expressed as mean ± SEM of 10 animals in each group. ** and *** denote $P < 0.01$ and 0.001, respectively, when comparing infected C3H/HeSnJ versus infected C57BL/6J mice.

NIH-PA Author Manuscript

NIH-PA Author Manuscript

NIH-PA Author Manuscript

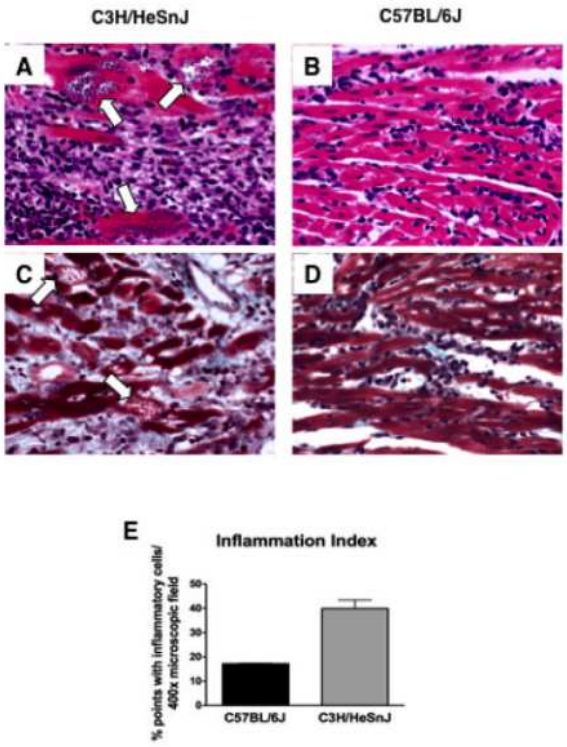

Figure 2. C3H/HeSnJ mice, but not C57BL/6J mice, develop severe fibrosing myocarditis and cardiac failure in the acute phase of infection with *T. cruzi*.

Hearts were collected 30 days after infection, and paraffin-embedded sections were stained with either Hematoxylin and Eosin (A, B) or Gomori's Trichrome stain (C, D). Representative images are shown for infected C3H/HeSnJ mice (A, C) and infected C57BL/6J mice (B, D). In panels A and C, arrows point to amastigote pseudocysts. Magnification, 400X. Data are representative of 5 mice/group from a single experiment performed at least 5 times with a similar pattern of results. E) Quantification of inflammation. Data are from a single representative experiment with 5 mice in each group. * $P < 0.05$.

NIH-PA Author Manuscript

NIH-PA Author Manuscript

NIH-PA Author Manuscript

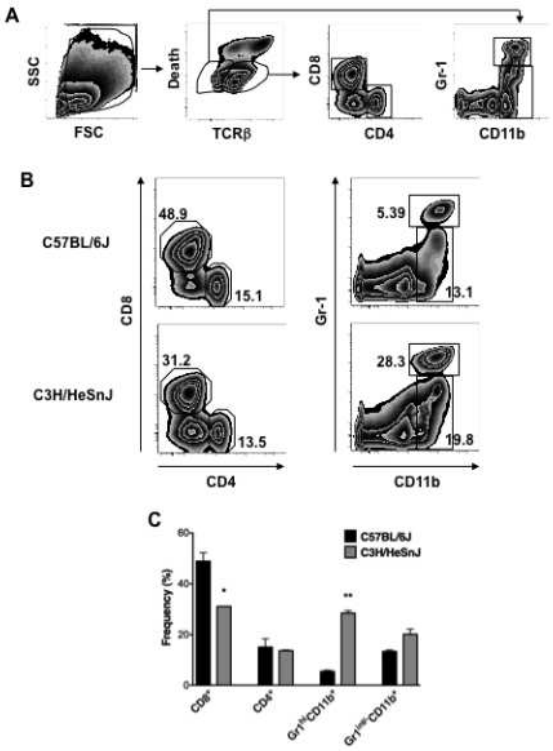

Figure 3. Myocardial infiltrates after *T. cruzi* infection have a higher frequency of Gr-1^{hi} CD11b^{+}TCR $^{-}$ cells, but a lower frequency of CD8^{+}TCR $^{+}$ cells in C3H/HeSnJ mice compared to C57BL/6J mice

A) Gating of leukocytes isolated from heart 28-30 days after infection. Death denotes staining with LIVE/DEAD (Invitrogen). B) Subset analysis in the heart: representative experiment of 2 experiments performed. Numbers correspond to the frequency of the adjacent gated population. The top two panels are for C57BL/6J mice, the bottom two for C3H/HeSnJ mice. C) Subset analysis: summary data. The frequency is shown for the indicated cell types in the heart of *T. cruzi*-infected C3H/HeSnJ (grey bars) or C57BL/6J (black bars) mice. Data represent mean ± SEM of 2 pools of 4-5 hearts in each group. * and ** denote $P < 0.05$ and 0.01, respectively, when comparing C3H/HeSnJ and C57BL/6J mice.

NIH-PA Author Manuscript
NIH-PA Author Manuscript
NIH-PA Author Manuscript

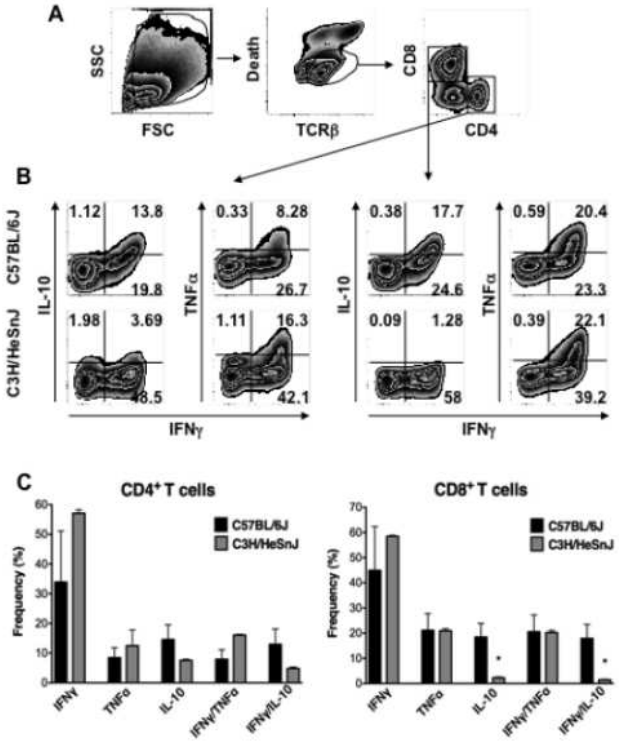

Figure 4. Detection of high frequencies of IL-10-producing effector T lymphocytes in hearts from C57BL/6J relative to C3H/HeSnJ mice 30 days after *T. cruzi* infection: flow cytometry analysis

The frequency of intracellular cytokine-expressing cells is shown for $CD8^+$ or $CD4^+$ T cell subpopulations isolated from the heart of *T. cruzi*-infected C3H/HeSnJ or C57BL/6J mice. A and B) A representative experiment of 2 performed is shown. A) Gating of myocardial leukocytes. Death denotes staining with LIVE/DEAD (Invitrogen). B) Intracellular cytokine analysis of the gated subpopulations indicated in the rightmost panel of part A. C) Summary data of 2 independent experiments. Bars represent means ± SEM of 2 pools of 5 hearts in each group. * for $P < 0.05$ when comparing C3H/HeSnJ and C57BL/6J mice.

NIH-PA Author Manuscript

NIH-PA Author Manuscript

NIH-PA Author Manuscript

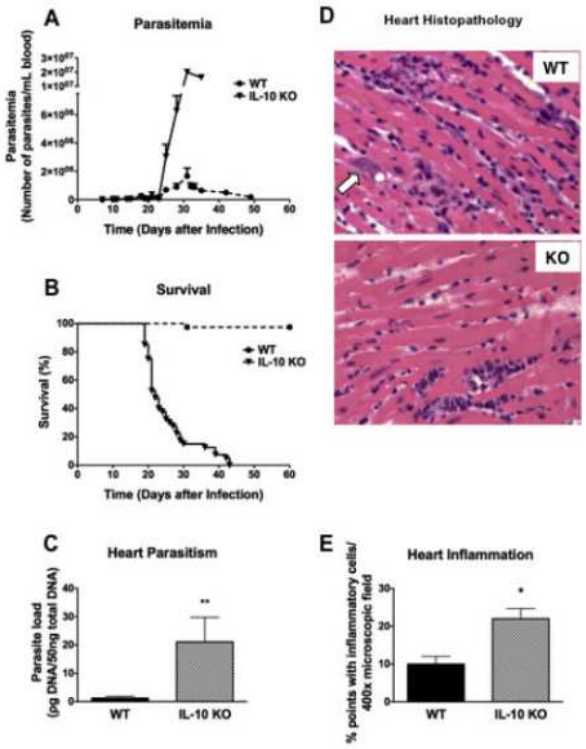

Figure 5. IL-10 is a strong resistance factor in a C57BL/6J model of *T. cruzi* infection

Wild type and IL-10$^{-/-}$ mice were infected with *T. cruzi* (Colombiana strain). A) Parasitemia. Data are the mean ± SEM summarized from seven independent experiments (total of n=40 animals per group). B) Survival. Data are presented as the summary of seven independent experiments, n=40 animals in each arm. $P < 0.0001$. C, Parasite burden in the heart on day 25 p.i. Data are the mean ± SEM from one experiment (n=5 per group). D, Histopathology in the hearts of infected IL-10 ko (top) and control mice (bottom) on day 25 p.i. Cardiac sections were stained with hematoxylin and eosin. Magnification = 400X. White arrow denotes amastigote pseudocysts. E) Quantification of inflammation. Data are based on one representative experiment with 7 IL-10 ko mice and 5 WT mice at day 20 pi. * $P < 0.05$.

NIH-PA Author Manuscript

NIH-PA Author Manuscript

NIH-PA Author Manuscript

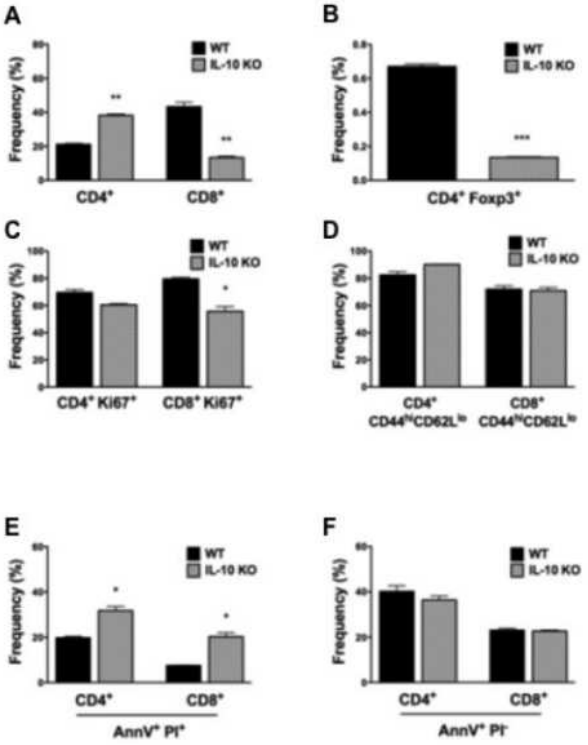

Figure 6. IL-10 deficiency skews distribution, proliferation and survival of T cells in the hearts of *T. cruzi*-infected mice

T cells were purified from hearts of the indicated mouse strains on day 18 post-infection with *T. cruzi* and analyzed by FACS with the markers indicated on the x-axis for CD4+ and CD8+ T cell distribution (A), Foxp3+CD4+ Treg distribution (B), T cell proliferation (C), T cell activation (D) and cell death (E, F). AnnV and PI denote Annexin V and propidium iodide, respectively. Data in A-D are from a single experiment performed. Data in E and F are from a single experiment performed separately from A-D. In all experiments, 10 mice were analyzed in each group. *$P < 0.05$; **$P < 0.01$; ***$P < 0.001$.

NIH-PA Author Manuscript

NIH-PA Author Manuscript

NIH-PA Author Manuscript

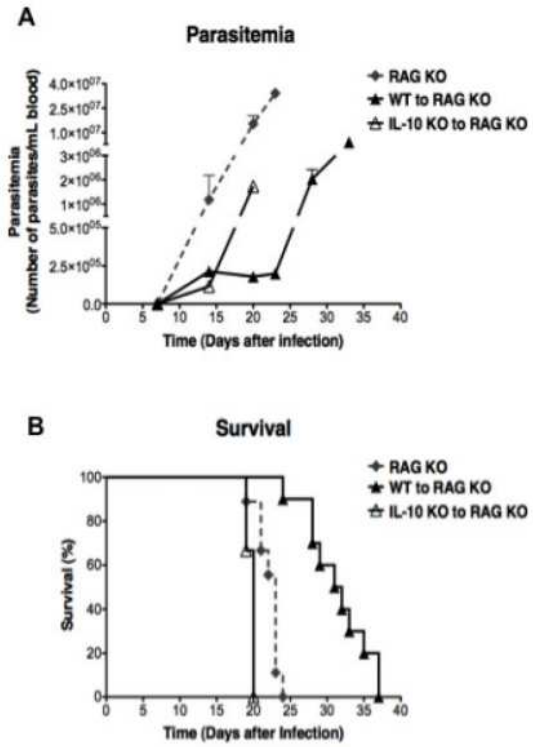

Figure 7. Adoptive transfer of IL-10$^{+/+}$, but not IL-10$^{-/-}$, CD3^{+} T cells confers partial resistance to *T. cruzi*-infected RAG-1 deficient mice

CD3^{+} T cells were isolated and sorted from spleens and lymph nodes from naive WT or IL-10 KO mice and a total of 2 × 10^{6} cells were injected IV into RAG-1 deficient mice as indicated in the inset. The animals were then infected with 1000 *T. cruzi* blood stage trypomastigotes 24 hrs later. A) Parasitemia. B) Survival. Data are summarized from two independent experiments (total of n=10 animals per group), and are presented as the mean ± SEM. In panel B, $P < 0.0001$, when comparing (WT to RAG KO) vs RAG KO, or (WT to RAG KO) vs (IL-10 KO to RAG KO). P=0.0008, when comparing RAG KO vs (IL-10 KO to RAG KO).

NIH-PA Author Manuscript NIH-PA Author Manuscript NIH-PA Author Manuscript

Table I

Histopathological evaluation of organs from T. cruzi-infected C3H/HeSnJ or C57BL/6J mice 28-31 days p.i.

Ten C3H/HeSnJ and 7 C57BL/6J mice were either found dead or were euthanized after fulfilling protocol criteria for euthanasia 28-31 days p.i.; organs were paraffin-embedded and stained with hematoxylin and eosin. Scoring: − Not present, + Minimal; ++ Mild; +++ Moderate; ++++ Severe. EMH: Extramedullary Hematopoiesis.

	Heart						Spleen	Liver
Strain	Inflammation	Thrombosis	Fibrosis	Myodegeneration or necrosis	Parasitism	Mineralization		
C3H/HeSnJ	+++ Multifocal, Primarily lymphocytic, Interstitial, Inflammation obscures nests	Endocardial, in right atrium and/or right ventricle, presence of neutrophils	+++	++++ Multifocal	+++	Multifocal	Moderate EMH, moderate lymphoid hyperplasia	Mild EMH, Mild lipidosis
C57BL/6J	+ Multifocal, Primarily lymphocytic, Interstitial	−	++	+	+	−	Mild to moderate EMH, Mild to moderate lymphoid hyperplasia	Mild EMH

J Immunol. Author manuscript; available in PMC 2013 January 15.

NIH-PA Author Manuscript

NIH-PA Author Manuscript

NIH-PA Author Manuscript

Table II

Differential expression of pro-inflammatory, immunoregulatory and antimicrobial factors in hearts of C57BL/6J and C3H/HeSnJ mice 30 days after T. cruzi infection: Quantitative RT-PCR analysis

Data are the average of 5 samples for each factor normalized to HPRT and expressed as a fold-change compared with heart RNA from uninfected isogenic control mice. Bolded factors were differentially expressed in C3H/HeSnJ vs C57BL/6J. *, ** and *** denote $P < 0.05$, 0.001 and 0.001, respectively.

		C3H/HeSnJ	C57BL/6J
Chemokines	Cxcl1	6.1 ± 1.9	5.3 ±0.5
	Cxcl2	**61.6 ± 27.9***	**5.5 ± 0.9**
	Cxcl9	**435.3 ±14.6*****	**75.4 ± 6.4**
	Cxcl10	173.1 ±49.8	94.5 ±5.5
	Cxcl11	**552.3 ± 202.3***	**16.7 ± 1.9**
	Cxcl16	16.9 ± 3.3	11.2 ± 1.3
	Ccl2	**104.3 ± 0.9****	**40.4 ± 6.3**
	Ccl3	165.8 ± 27.7	104.3 ± 11.1
	Ccl4	1390.3 ±372.0	983.7±173.8
	Ccl5	**482.8 ± 57.8**	**843.6 ± 82.0***
	Ccl7	**37.3 ± 10.0***	**10.3 ± 0.7**
	Ccl20	29.4 ± 13.0	8.1 ±2.4
	Xcl1	**15.1 ± 1.8***	**9.1 ± 0.8**
	Cx_3cl1	**12.1 ± 3.8***	**3.0 ± 0.4**
Chemoattractant Receptors	Cxcr1	142.7 ± 83.9	19.4 ±6.4
	Cxcr2	37.1 ±20.8	6.7 ±2.1
	Cxcr3	**220.4 ± 105.7***	**10.3 ± 0.8**
	Ccr1	**107.0 ± 48.0***	**5.7 ± 2.3**
	Ccr2	**35.2 ± 2.9*****	**9.0 ± 0.9**
	Ccr3	**13.0 ± 5.2***	**1.1 ± 0.3**
	Ccr4	**22.6 ± 11.0***	**1.7 ± 0.5**
	Ccr5	106.0 ± 53.5	16.8 ±0.9
	Ccr6	**24.9 ± 12.0***	**1.5 ± 0.5**
	Ccr7	15.6 ± 9.4	3.7 ± 1.0
	Xcr1	**3.3 ± 0.6***	**1.6 ± 0.1**
	Cx_3cr1	13.7 ± 8.1	9.1 ±0.7
	Fpr1	29.9 ± 12.5	10.2 ± 1.4
	D6	**7.3 ± 2.5***	**1.9 ± 0.4**
Cytokines	IL-1p	73.3 ±43.7	29.0 ±4.4
	IL-4	12.0 ±5.7	2.3 ±0.6
	IL-10	**23.3 ± 2.0**	**203.5 ± 32.8***
	IL-12 p40	**152.9 ± 72.4**	**310.9 ± 23.5***
	IL-13	**43.3 ± 22.3***	**2.1 ± 0.6**
	IL-17A	**20.6 ± 7.5***	**3.5 ± 1.0**

NIH-PA Author Manuscript

NIH-PA Author Manuscript

NIH-PA Author Manuscript

		C3H/HeSnJ	C57BL/6J
	IL-21	77.5±7.9	14.1 ±2.6
	IL-22	124.4 ± 58.0	24.7 ±7.1
Other factors	**Arg-1**	**1890.0 ± 484.2****	**198.2 ± 66.6**
	NOS 2	**97.2 ± 29.0***	**13.4 ± 2.8**
	T-bet	**11.2 ± 3.4***	**3.9 ± 0.3**
	Gata-3	**6.9 ± 2.1***	**2.7 ± 0.2**
	Foxp3	21.4 ± 9.6	4.1 ± 1.3